DOI 10.5162/sensoren2024/D5.4

Development of an Optimization Tool for Advanced Magnet Design in Sensor Accuracy Enhancement for Automotive Application

Jie Zhou, Markus Dietrich, Florian Zeller, Wai-Wai Buchet
Schaeffler Automotive Buehl GmbH & Co. KG, Buehl/ Industriestr. 3, 77815 Bühl/Germany
E-Mail: {jie.zhou, markus.dietrich, florian.zeller, wai-wai.buchet}@schaeffler.com

Abstract:
This paper introduces a novel optimization tool designed to enhance sensor accuracy in automotive applications by determining the optimal dimensions and positioning of an axially magnetized cylindrical magnet used in magnetic linear sensors. Utilizing both the Finite Element Method and analytical equations, the study evaluates the impact of magnet properties on sensor performance, focusing on resolution and nonlinearity characteristics. Through comprehensive multivariate optimization, considering the constraints, optimal magnet configurations are identified, improving sensor accuracy and cost-effectiveness. The methodologies presented extend to various sensor types, offering a scalable approach to magnet design in e-mobility.

Kurzfassung:
Dieser Beitrag stellt ein neuartiges Optimierungswerkzeug vor, das für die Verbesserung der Sensorpräzision in Automobilanwendungen entwickelt wurde, indem es die optimalen Dimensionen und Positionierungen von einem axial magnetisierten permanenten Magneten bestimmt, die in magnetischen Linearsensoren verwendet werden. Unter Einsatz der Finite-Elemente-Methode und analytischer Gleichungen bewertet die Studie den Einfluss der Magneteigenschaften auf die Sensorleistung, mit Fokus auf Auflösung und Nichtlinearität. Durch umfassende multivariate Optimierung, einschließlich Beschränkungen, werden optimale Magnetkonfigurationen identifiziert. Diese verbessern die Sensorpräzision und Kosteneffektivität erheblich. Die präsentierten Methoden lassen sich auf verschiedene Sensortypen erweitern und bieten einen skalierbaren Ansatz für Magnetdesign in der E-Mobilität.

Keyword: position sensor, multivariate optimization/ Pareto optimization, permanent magnet
Schlagwort: Positionssensor, Mehrzieloptimierung/ Pareto-Optimum, Dauermagnet

I. Introduction

In the rapidly evolving domains of e-mobility and autonomous driving, precise tracking of linear movements has become essential. These advancements necessitate enhanced sensor performance. Predominantly, magnetic technology is employed in linear sensors where a permanent magnet generates a magnetic field. A crucial factor in increasing sensor accuracy is the optimization of the magnet's dimensions and positioning for effective measurement. This study introduces a novel tool designed to determine the optimal dimensions and positioning of the magnet.

Sensor accuracy and cost are the two main factors requiring optimization. The accuracy of these sensors primarily depends on two characteristics of the sensor signals: resolution and nonlinearity. Resolution addresses stochastic errors, whereas nonlinearity pertains to systematic errors. Our position sensors predominantly utilize the Atan2-function for determining position. Hence, we leverage the properties of the Atan2-function to analyze both resolution and nonlinearity. Resolution is quantified through the Signal-to-Noise Ratio (SNR), defined as the ratio of the maximum magnetic field to the noise level, such as Earth's magnetic field [1]. Nonlinearity is evaluated using either Total Harmonic Distortion (THD) [2] or Most Significant Distortion (MSD) [3]. Both THD/MSD and SNR are influenced by the material properties (whether homogeneous or heterogeneous), the dimensions of the permanent magnet (notably the length-diameter ratio, or LD-factor) [4], and the positioning of the magnet. This analysis aims to explore how these parameters respond to variations, highlighting their sensitivity and establishing relationships between input parameters and optimization objectives. Subsequently, a multivariate optimization problem is formulated and addressed.

II. System Parameter Determination

A variety of magnet types can be utilized in sensor applications; for initial investigations, an axially magnetized cylindrical magnet is selected (See Fig. 1a). This configuration is pivotal for further examination due to its relevance in linear movement tracking.

II.a Magnetic Field Calculation Methods

Two primary methods are employed to calculate the properties of the magnet: the Finite Element Method (FEM) and analytical equations.

- FEM: As depicted in Fig. 1b, FEM requires a homogeneous and extremely fine mesh to achieve the desired accuracy for THD/MSD analysis. Although it provides comprehensive magnetic field data for each simulation, it demands a high computational load, necessitating up to 1000 simulations for robust sensitivity analysis. To expedite calculations, a model order reduction method is applied, which still requires at least 50 FEM simulations for high-precision analyses [5,6].

- Analytical Equations: The analytical approach involves equations (1-3) derived from the methodologies introduced in [4], which are less computationally intensive and offer high accuracy. These equations compute the magnetic field components B_r, B_θ and B_z at any given point (r,θ,z) in cylindrical coordinates, as defined below:

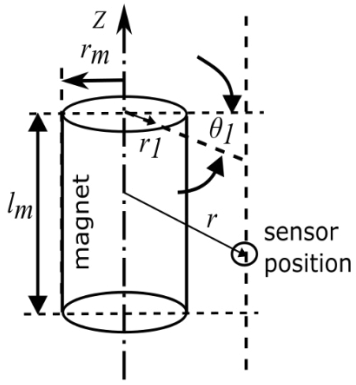

a) Sketch of sensor magnet

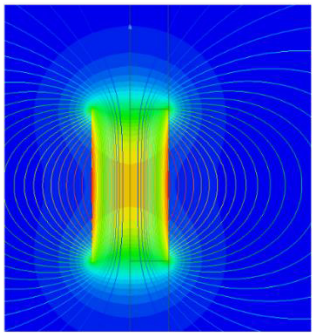

b) FEM result of sensor magnet

Fig 1: axially magnetized cylinder magnet

$$B_r = \frac{B_{rem}}{4\pi}\sum_{i=1}^{2}(-1)^{i+1}\int_0^{r_M}\int_{-\pi}^{\pi} r1\,[r - r_1\cos(\theta-\theta_1)]G^3 d\theta_1 dr_1 \quad (1)$$

$$B_\theta = \frac{B_{rem}}{4\pi}\sum_{i=1}^{2}(-1)^{i+1}\int_0^{r_M}\int_{-\pi}^{\pi} r_1^2\sin(\theta - \theta_1)\,G^3 d\theta_1 dr_1 \quad (2)$$

$$B_z = \frac{B_{rem}}{4\pi}\sum_{i=1}^{2}2\,(-1)^{i+1}\int_0^{r_M}\int_{-\pi}^{\pi}[z - z1]G^3 d\theta_1 dr_1 \quad (3)$$

Where B_{rem} represents the remanent magnetization and G (the Green's function for the cylindrical coordinate system) is defined as [4,7]:

$$G(r,\theta,z,r_1,\theta_1,z_1) = [r^2 + r_1^2 - 2rr_1\cos(\theta-\theta_1) + (z-z_1)^2]^{-\frac{1}{2}} \quad (4)$$

II.b Comparison of Methods

Both FEM and analytical equations yield similar results; however, for the continuation of this study, only analytical equations will be utilized due to their efficiency and lower computational demand.

The given problem is axial symmetrical, the calculation therefore only should focus on the radial (B_r) and axial (B_z) magnetic fields, presented in Fig. 2., where the parameter α for the x-axis represents the relative radial distance, which is defined as:

$$\alpha = \frac{\mathrm{r}}{\mathrm{r_M}} \quad (5)$$

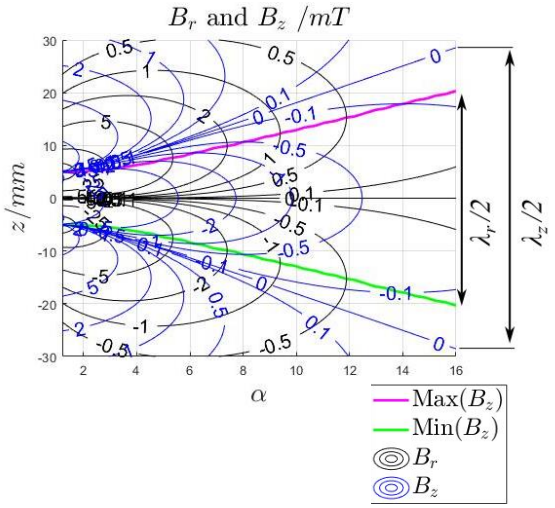

Fig 2: Br and Bz of a cylinder magnet

The fields are sinusoidal along the z-axis, with varying wavelengths (λ_r and λ_z), which can introduce additional positional measurement errors. To account for this, a new parameter Ω is defined to evaluate and minimize this discrepancy:

$$\Omega = \frac{\lambda_r}{\lambda_z} - 1 \tag{6}$$

II.c Further Analysis and Optimization

In subsequent analyses, the magnitudes of the magnetic fields and their Total Harmonic Distortion (THD) are computed for various positions and input parameters, as summarized in Fig. 3. A key geometric parameter, the LD-factor (β), is introduced:

$$\beta = \frac{r_M}{l_M} \tag{7}$$

Maps in Fig. 3 and Fig. 4 aid in constructing objective functions for optimizing sensor accuracy: $f_{\hat{B}r}$, $f_{\hat{B}z}$, f_{THDr}, f_{THDz} and f_{Ω}. For efficient applications, values in maps a) and b) are normalized with Brem, and are unitless.

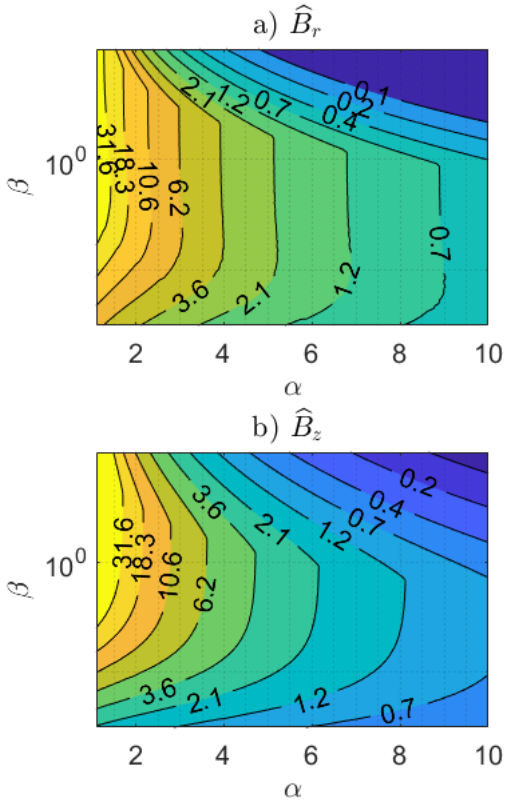

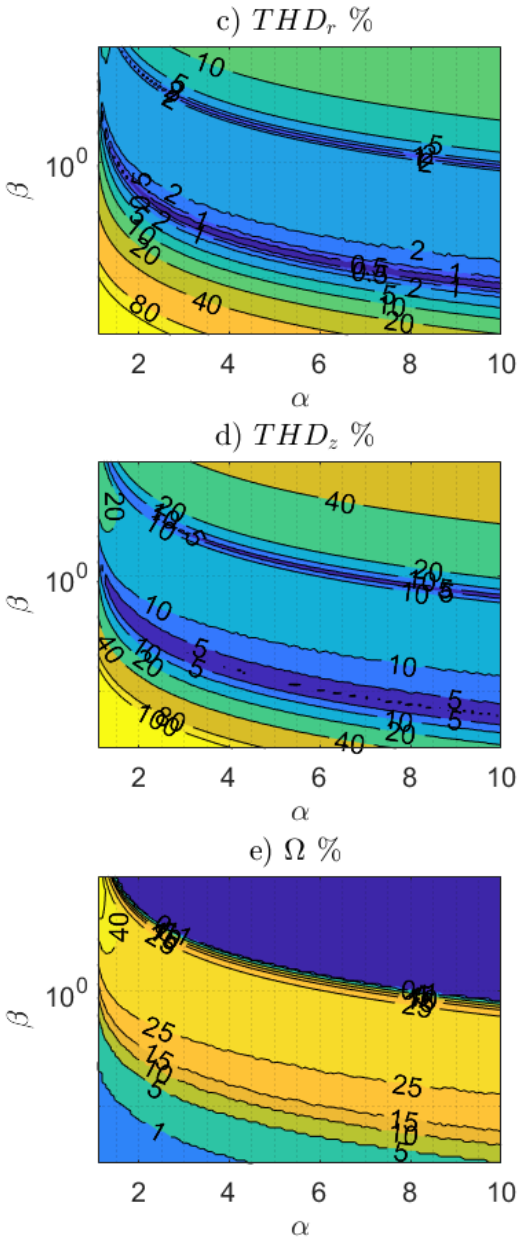

Fig 3: Magnitudes, THD and Ω of a cylinder magnet

For cost optimization, the objective function f_{cost} is formulated as follows, incorporating the material-dependent variables of unit price p and density ρ:

$$f_{cost} = p(B_{rem}) \cdot \rho(B_{rem}) \cdot \pi \cdot r_M^2 \cdot l_M \tag{8}$$

This function aims to minimize the cost by evaluating different material choices based on their price per unit volume. The parameters p and ρ depend on the type of magnet material used and are detailed in Table 1.

	B_{rem} /T	p /$/kg	ρ /kg/m³
NdFeB sintered	1.2	70.00	7500
SmCo	1.0	95.00	8300
NdFeB bonded	0.8	91.00	5950
Ferrite	0.3	6.40	7300

Tabel 1: Unit price and density of different materials [8]

III. Optimization

The objective functions for various signal and cost aspects were defined previously. To determine the optimal solution comprehensively, we consider two methodologies[10].:

a) Step-by-Step Optimization: This method involves sequentially optimizing one aspect at a time, using the results from the previous aspect as a baseline. This approach is visually represented in Fig. 4, where the color-coded areas indicate regions of optimum performance for next optimization steps.

b) Composite Objective Function: Alternatively, a composite objective function can be constructed, aggregating individual objective functions weighted by their respective importance:

$$f_{total} = \sum_{i=1}^{n} w_i \cdot f_i^2 \qquad (9)$$

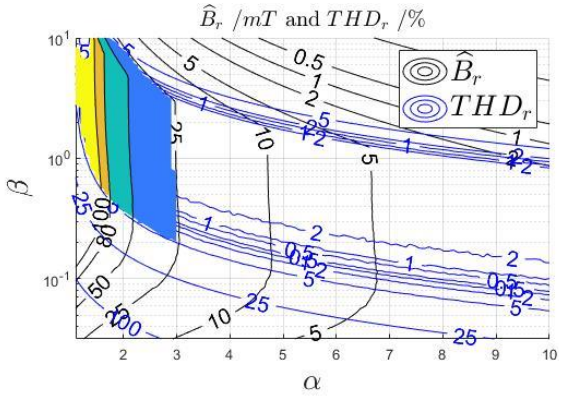

Fig 4: Step-by-Step optimization

Here, w_i denotes the weight assigned to the different objective function, reflecting its relative priority [10].

III.a Complexity and Computational Methods

For complex systems where the relationships between parameters are highly nonlinear, the step-by-step method might be simplistic. In such cases, constructing a new and summed objective function using the Karush–Kuhn–Tucker (KKT) conditions is preferable. However, due to the extreme nonlinearity and the inability to fit the maps to closed formulas, interpolation methods [10] are recommended. Prior to interpolation, it is essential to smooth the maps (see Fig. 5) to eliminate numerical errors and local minima that could degrade optimization performance. Techniques such as Fast Fourier Transform (FFT) based filtering [7] and 2D-moving averages have been explored; while FFT was ineffective in reducing local minima, moving averages proved useful in smoothing without altering critical areas of the map.

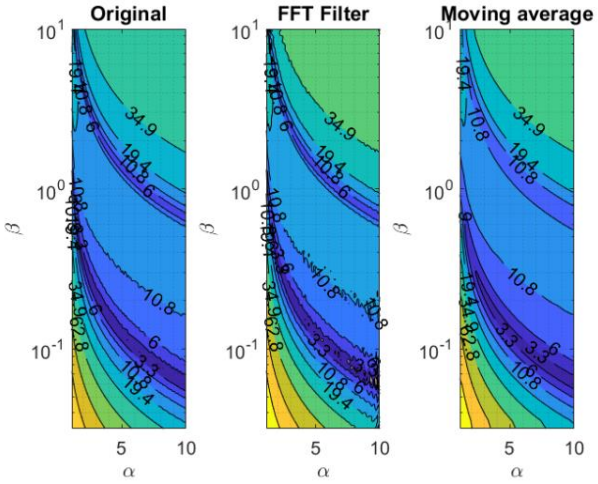

Fig 5: Smoothing of the map

III.b Transformation and Normalization of Objective Functions

The objective functions $f_{\hat{B}r}$ and $f_{\hat{B}z}$, being concave, shall be transformed into convex forms to facilitate optimization (see SNR in [1]):

$$f^*_{\widehat{B_r}} = log_2\left(\frac{B_{Earth}}{f_{\widehat{B_r}}}\right) \quad \text{and} \quad f^*_{\widehat{B_z}} = log_2\left(\frac{B_{Earth}}{f_{\widehat{B_z}}}\right) \qquad (10)$$

Normalizations are important when combining all objective functions together for (9), as it ensures that disparate magnitudes do not skew the aggregated objective function. The normalization factor and the weights w_i may be chosen intuitively or derived from systematic methods such as using inverses of mathematical sequences like Fibonacci, prime numbers, or Lucas numbers [11], to balance their scaling effects.

III.c Constraints and Global Optimization

To enhance stability and feasibility, constraints are imposed: the resolution (inverse of SNR) should be less than 1° [1], and THD should be below 5% [2]. Additionally, while seeking the global minimum of the optimization landscape, it's prudent to initiate the search from multiple random starting points across the entire range of parameters. This strategy mitigates the risk of converging to local minima and ensures a more comprehensive exploration of potential solutions [9].

IV. Results

The effective measuring range, as observed from Fig. 2, is approximately half of the magnet's length. Consequently, we evaluated a measuring range with a span of 5 mm to determine the optimal magnet radius, measuring radius and associated costs. The results indicate that NdFeB is the most suitable material for this application, with the optimal magnet radius and position highlighted in a THD map (See Fig. 6a). In the scenario labeled “equal,” which does not utilize weighted values, significant disparities were noted compared to other scenarios.

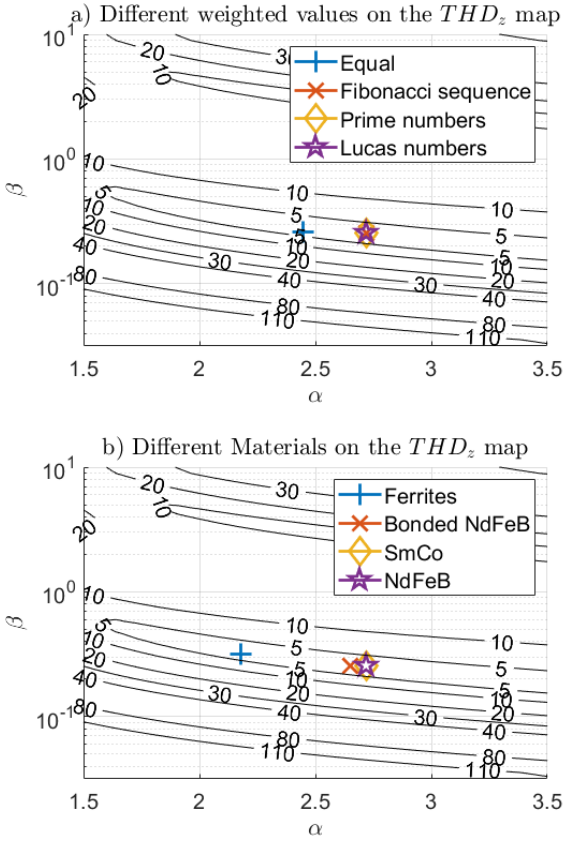

Fig 6: Optimization result

Additional testing with specified material and consistent weighted values were performed. The outcomes, as shown in Fig. 6b, reveal that the measuring position of a Ferrite magnet is positioned closer relative to other materials, achieving better resolution to satisfy the constraint conditions. Conversely, the measuring distance for a NdFeB magnet is greater, potentially offering comparable resolution to the Ferrite magnet but with reduced nonlinearity.

V. Discussion and outlook

This study outlines methods for optimizing the geometry and material of axially magnetized cylindrical magnets for linear position sensing and demonstrates how to pinpoint optimal measuring positions. Although sensor accuracy is primarily influenced by the magnet's properties, external factors such as temperature, drift effects, and cost also play critical roles. These elements can be integrated into our optimization framework to refine the methodology further. Additionally, exploring different magnet shapes and extending the approach to rotational position applications could broaden the tool's applicability. Future work will focus on incorporating more complex variables like environmental impacts to enhance the robustness and utility of sensor technologies in e-mobility.

VI. Reference

[1] J. Zhou, M. Dietrich, P. Walden, J. Kolb, and M. Doppelbauer, "The resolution of atan2 function", 2020 IEEE Sensors, pp. 1–4. (2020); DOI: 10.1109/SENSORS47125.2020.9278722

[2] J. Zhou, M. Dietrich, P. Walden, J. Kolb, M. Doppelbauer, "Online harmonic error compensation of Atan2 function for a low-cost automotive sensor application", tm - Technisches Messen, vol.0, no.0, (2021); DOI: 10.1515/teme-2021-0038

[3] J. Zhou, M. Dietrich, F. Zeller; W. Buchet, " Enhancing Positioning Sensor Applications: Online Harmonic Order Determination of Atan2-Function", 2023 IEEE Sensors, pp. 1–4. (2023); DOI: 10.1109/SENSORS56945.2023.10325075

[4] E. P. Rurlani, "Permanent Magnet and Electromechanical Devices: Materials, Analysis, and Applications", Academic Press, (2001); DOI: 10.1016/B978-012269951-1/50005-X

[5] Dynardo GmbH, "Methode for multi-disciplinary optimization and robustness analysis", (2019)

[6] Z. Qu MOR, "Model Order Reduction Techniques with Applications in Finite Element Analysis", Springer (2013), DOI:10.1007/978-1-4471-3827-3

[7] S. Brunton, J. N. Kurtz, "Data-Driven Science and Engineering: Machine Learning, Dynamical Systems, and Control", Cambridge University (2022); DOI: 10.1017/9781108380690

[8] Magnet material price, online resource: https://allianceorg.com/commodity-prices/magnet-and-material-costs/, (April. 01. 2024)

[9] J.Sobieszczanski-Sobieski, A. Morris, M.Tooren " Multidisciplinary Design Optimization Supported by Knowledge Based Engineering", Wiley (2015); DOI: 10.1002/9781118897072

[10] F. P. León" Messtechnik: Grundlagen, Methoden und Anwendungen", Springer (2019); DOI: 10.1007/978-3-662-59767-5

[11] T. Koshy, "Fibonacci and Lucas Numbers with Applications (Pure and Applied Mathematics: A Wiley Series of Texts, Monographs and Tracts", Wiley (2019); DOI: 10.1002/9781118033067